A Method for Prediction of In-situ Stress Based on Empirical Formula and BP Neural Network

Chuan-gang Xiang[1(✉)], Bo Chi[1], and Shu-yan Sun[2]

[1] Exploration and Development Research Institute of Da Qing Oilfield Co. LTD, Daqing, China
{xiangchuangang,chibo}@petrochina.com.cn
[2] Daqing Oilfield Drilling Engineering Company, Daqing, China
sunshuyan@petrochina.com.cn

Abstract. To solve the problems of complex in-situ stress of tight sandstone reservoir, few sample points of experimental data, difficulty in in-situ stress prediction, etc., a method for one-dimensional, two-dimensional and three-dimensional in-situ stress prediction based on geomechanics and BP neural network was innovatively proposed by comprehensively using various data such as core data, mechanical experimental data, logging data, etc. In this method, the rock mechanics parameters of single well in the study area were predicted by neural network method using the logging data as the learning sample and measured rock physical parameters as the monitoring data first; then the in-situ stress of single well was accordingly calculated by empirical formula, and predicted and analyzed by neural network algorithm using the calculated in-situ stress of single well selected by error analysis and the indoor measured in-situ stress as the monitoring data and the conventional logging data as the learning samples. The application in the actual areas shows that the predicted results of in-situ stress not only conform to the measured data, but also follow the logging curves, and thus provide an important basis for the design of integrated geological engineering scheme.

Keywords: BP neural network · error analysis · sample expansion · geostress prediction · Integration of geology and engineering

J. Lin (Ed.): IFEDC 2023, SSGG, pp. 485–497, 2024.
https://doi.org/10.1007/978-981-97-0272-5_41

1 Introduction

With increasing difficulty in conventional energy exploitation, tight sandstone reservoirs have gradually become one of the important exploration and development targets [1–3]. Due to their low porosity and low permeability, they are mainly developed by horizontal drilling and staged fracturing, for which the current in-situ stress state is the main controlling factor [4–6]. In fracturing, the in-situ stress state controls the shape, height, width and direction of hydraulic fractures, and affects the fracturing stimulation effect. Also, in-situ stress is an important basis for well pattern deployment and adjustment and lateral segment direction selection. Therefore, the evaluation of the current in-situ stress is very important for the exploitation of tight sandstone reservoirs [7, 8].

Stress activity causes rock deformation or fracture and plays an important role in oil and gas exploration and development (Jenkins, 2017). The in-situ stress is generally composed of tectonic stress, gravity stress, thermal stress, pore pressure, etc., and its state is usually represented by three normal stresses, the maximum horizontal principal stress (σ H), vertical stress (σ v) and minimum horizontal principal stress (σ h) (Lin et al., 2006; Kuuskraa and Ammer. 2004; Matsuki and Takeuchi. 1993) [9, 10]. The magnitude and direction of in-situ stress in different strata in different regions in the crust change with space and time to form an in-situ stress field. Nowadays, there are many methods for evaluation of in-situ stress, such as hydraulic fracturing, acoustic emission and logging calculation. The methods are commonly used to determine the in-situ stress. Fracturing method refers to the calculation of the in-situ stress according to the relationship of fracturing pressure and time. The hydraulic fracturing method is reliable, direct and simple, but not all wells have small-scale fracturing test data in actual production. Acoustic emission method (Goodman 1963) refers to the determination of in-situ stress according to the characteristics of elastic waves in the form of which some energy is released from the rocks when the rocks are compressed by external forces [11]. By analyzing the acoustic characteristics of these elastic waves, the size of in-situ stress can be obtained. The acoustic emission method can measure the stress in the deep reservoirs, but has high costs of acoustic emission test, uncontinuity of results, and few sample points of indoor measured data and roughly estimates the in-situ stress state of the untested reservoirs. The logging curve-based formulas method overcomes the shortcomings of high test price and discontinuous measuring points. It refers to the method of indirect calculation of in-situ stress according to the formula after the logging data are used to calculate the rock mechanics parameters, such as formation Poisson's ratio, Young's modulus, shear modulus and bulk modulus, etc. However, the calculation process cannot be directly calibrated by the indoor experimentally measured in-situ stress results [12], and there is a large error between final calculation results and the measured data always [13, 14]. The neural network method better overcomes the disadvantage that the indoor experimentally measured in-situ stress results cannot be used for logging calibration, and seeks the relationship between the indoor experimentally measured in-situ stress results and the geophysical logging curve by machine learning. However, the relationship will be supported by a large number of the indoor experimentally measured in-situ stress results [15].

To solve the above problems, the data point continuity of logging curve-based formulas method and the advantages of data calibration of BP neural network method were combined to further improve the accuracy of in-situ stress prediction.

It includes the following steps: (1) The geophysical logging parameters of tight sandstone oil and gas wells, X-MAC logging parameters, indoor experimentally measured rock parameters and stress value parameters were acquired; (2) The standard layer statistical analysis method was used for environmental correction, and the histogram method was used to standardize the data of tight sandstone oil and gas wells; (3) The location correction method was used to correct the depth data used during the acquisition of the above data; (4) Linear regression method was used to predict the data of S-wave curve according to X-MAC logging parameters and processed geophysical logging parameters of the area; (5) According to the predicted S-wave slowness, geophysically logged P-wave slowness and density logging parameters, the dynamic Young's modulus and dynamic Poisson's ratio of rock were calculated jointly; according to the indoor experimental data, the rock mechanics parameters calculated according to the logging data were dynamically and statically corrected to obtain static Young's modulus, static Poisson's ratio, etc.; (6) according to the indoor experimentally measured data, the biot coefficient and pore pressure were obtained by fitting, and combined with the static rock mechanics parameters to calculate the vertical stress, maximum horizontal stress and minimum horizontal stress; and the error of the indoor experimentally measured stress data was analyzed; (7) the calculated in-situ stress of the wells with small errors was used to extend the indoor experimentally measured in-situ stress data of small samples to form large sample learning data; and the geophysical logging parameters of single wells were used as training samples to calculate the vertical in-situ stress, maximum horizontal stress and minimum horizontal stress of tight sandstone oil and gas wells by neural network method; (8) a geological mesh model was created to spatially interpolate geophysical logging parameters, and a three-dimensional in-situ stress field model was obtained based on neural network method to predict, analyze and evaluate the spatial in-situ stress distribution of tight sandstone reservoirs.

2 Sample and Experiment

A tight sandstone reservoir in Sanzhao Sag in the north of Songliao Basin was taken as an example. It has large depth, strong diagenesis, relatively tight lithology, active porosity of 13.5%, and air permeability of $0.9 \times 10{-}3\ \mu m^2$. The natural gamma-ray logging curve of the whole well section shows "sandstone in mudstone", and the natural gamma-ray logging curve shows typical "sandstone-mudstone formation". The channel fill deposit and delta front deposit, especially anastomosing river flooding basin, mainly develop. The natural gamma-ray logging curves mainly show a dentate clock with medium/high amplitude, box, and small sawtooth with low amplitude. The data used were the logging data of 5 wells (G1, G2, G3, G4, and G5) in the area. There were 8 logging curves in total, including natural gamma-ray logging curve, natural potential curve, deep lateral resistivity curve, deep lateral resistivity curve, apparent resistivity curve, borehole diameter, density curve, and P-wave slowness curve. The reservoir more than 3550 m deep from the surface to underground was sampled at the

interval of 0.125 m. In addition, G2 well has X-MAC logging data, including S-wave slowness, P-wave slowness, etc.

The standard layer statistical analysis method was used for environmental correction. The relationship between the target curve and the reference curve of the standard layer was statistically analyzed by using one or more logging curves less affected by the borehole as the generating curves (reference curves) and the curve to be corrected as the target curve. The correlation between the generating curve and the target curve was established for the non diameter-expanded section to predict the target curve of the trans-well section to be corrected. The multiple regression analysis method was used to establish the functional relationship. The coefficients of each reference curve were obtained by solving the equation, and then the coefficients and reference curves were used to create a mathematical model. This method, which is to apply the mathematical model to obtain new curves in the borehole diameter-expanded section, comprises the following steps: (1) the data of the depth section beyond the target layer (30 m away from top or bottom) were removed, and only the data of the target layer of tight sandstone reservoir were remained for later data processing; (2) the lateral profiles of geophysical logging curves, such as diameter curve, gamma ray curve, P-wave slowness curve and density curve of 5 wells, were plotted; (3) the wells or depth sections with abnormal borehole diameters were found out through horizontal comparison, and the influences of borehole diameters on different curves were analyzed; and (4) and other curves of the depth sections with large error at the expanded diameter were reconstructed by empirical formula or linear relationship using one or more logging curves less affected by the borehole as the generating curve.

The linear correlation analysis based on the data of other wells except G5 shows that the relationship between the logarithm of P-wave slowness and the logarithm of density is not very linear, while the relationship between the logarithm of P-wave slowness and the logarithm of natural gamma-ray logging data is very linear. The P-wave slowness curve was corrected for the diameter-expanded section of G5 well by the established linear relationship.

Histogram method was used for standardization. The frequency histogram of each logging curve in the standard layer of each well in the study area was plotted first, and then the histogram of other wells was compared with the histogram of a coring well or specific well as the standard histogram. If both of them have the same value and similar shape, their scales are accurate. If they are very different and their standard layers have consistent lithology, their scales are inaccurate, and the difference in response value between their standard layer and the standard layer of the coring well is the correction value.

In the area, 5 wells were tested by uniaxial compression and triaxial rock mechanics experiment. The depth at which the indoor experimentally measured data were acquired was corrected by the location correction method. In this method, a bar chart was plotted based on the indoor experimentally measured data and compared with the trend of the logging curve at the same depth. In case of the best agreement, the upward and downward movement distance of the core was the corrected core location value; a bar chart was plotted based on the measured core density and compared with the logging curve at the same depth. In case of the best agreement, the core movement was taken as the corrected

location value. The location correction method can show the location depth difference intuitively. According to the above method, the indoor experimentally measured depth of the cores from 5 coring wells in the area was corrected for depth location, with the adjustment rate of 2.33%. The depth was not greatly corrected, with the average of 0.5 m and maximum of 1.2 m, within the allowable error range.

As shown in Fig. 2, the S-wave data calculation formula of tight sandstone in this area was established by linear regression between the S-wave slowness curve and the P-wave slowness curve of G2 well undergoing the X-MAC logging of Q1–Q7 layers. The regression equation has the calculation error of R2 = 0.897, indicating high correlation, so it can be used as a reference for calculation of the S-wave slowness curve data of other wells without X-MAC logging data. The S-wave slowness is calculated according to the following formula:

$$\Delta t_s = 51.142 \times e^{0.0121 \times \Delta t_p} \tag{1}$$

where △ts and △tp are the S-wave slowness and P-wave slowness, respectively.

The data of the S-wave slowness curve of Q8–Q9 layers of G2 well were used as posterior data for error analysis. The results show that the S-wave predicted by linear regression is highly consistent with the measured S-wave, with the relative error of predicted S-wave slowness within 2%, indicating that the data of the S-wave slowness curve are so reliable as to provide a basis for calculation of tight sandstone reservoir rock parameters in the next step.

According to the different methods for their acquisition, the rock mechanics parameters are divided into two types, static parameters, which are obtained from uniaxial or triaxial loading tests of rock samples in a laboratory, and dynamic parameters, which are the mechanical parameters under various dynamic loads or periodically varying loads (such as acoustic, impact, vibration, etc.) calculated according to the data of the logging curve.

According to P-wave and S-wave propagation equations, the theoretical relationship between P-wave and S-wave velocity and dynamic rock parameters was given; the P-wave slowness Δtp and S-wave slowness Δts was obtained from the logging data; and the bulk density ρ was obtained from the density logging data in order to calculate various rock mechanics parameters, including dynamic Young's modulus E, bulk modulus K, shear modulus G, and dynamic Poisson's ratio μ.

The e dynamic Young's modulus E is calculated according to the following formula:

$$E = \frac{\rho}{\Delta t_s^2} \frac{3\Delta t_s^2 - 4\Delta t_p^2}{\Delta t_s^2 - \Delta t_p^2} \tag{2}$$

where ρ represents the bulk density.

The dynamic Poisson's ratio, μ, is calculated according to the following formula:

$$\mu = \frac{1}{2} \frac{\Delta t_s^2 - 2\Delta t_p^2}{\Delta t_s^2 - \Delta t_p^2} \tag{3}$$

The shear modulus, G, is calculated according to the following formula:

$$G = \frac{\rho}{\Delta t_s^2} = \frac{E}{2(1+\mu)} \tag{4}$$

The bulk modulus, K, is calculated according to the following formula:

$$K = \rho \frac{3\Delta t_s^2 - 4\Delta t_p^2}{3\Delta t_s^2 \Delta t_p^2} = \frac{E}{3(1-2\mu)} \tag{5}$$

The deformation and rupture process of rock is slow and static. Before analysis of all rock mechanics, it is necessary to determine static parameters in order to predict the deformation and rupture of rock.

The elastic modulus directly calculated according to acoustic wave and density data is dynamic and thus impossible to predict the static mechanical properties of rocks. It is necessary to use a conversion formula obtained by laboratory data analysis to convert (generally linearly) the dynamic elastic modulus into static modulus, as shown in Fig. 3, so as to dynamically and statically correct the dynamic rock mechanics parameters calculated according to the logging data. According to the corrected static rock parameter results, the rock parameter profile of single well was plotted. It can be seen from Fig. 4 that the calculated static Young's modulus of G1 well is similar to the acoustic logging curve and density logging curve, and the static Poisson's ratio curve is negatively correlated to the acoustic logging curve and density logging curve, consistent with the trend of indoor experimentally measured data, indicating that the calculation result reflects the rock mechanical properties of the reservoir very well. According to the calculation results, the rock parameters of each single well in the study area can be evaluated.

The vertical stress, maximum horizontal stress and minimum horizontal stress of 5 wells in the study area were calculated according to the data of the density logging curve and static rock parameters. The number of experimentally measured in-situ stress values is too limited to obtain a continuous in-situ stress profile. However, the logging data have good continuity and high resolution, so it is very easy to popularize the method for prediction by empirical formula and BP neural network.

First of all, the data of the density logging curve were used to calculate the integral of formation thickness and density and further obtain the vertical in-situ stress. The calculation formula is as follows:

$$\sigma_{\mathrm{v}} = \int_0^{\mathrm{h}} \rho(h) g \cdot dh \tag{6}$$

where σv is vertical in-situ stress, MPa; h is the depth, m; ρ(h) is the density logging value, g/cm^3; g is the acceleration of gravity, m/s^2.

Then the formation pore pressure was calculated. In this embodiment, it was obtained by fitting the relationship between pressure and depth according to the indoor experimentally measured data.

Next, the biot coefficient was calculated. In this embodiment, it was obtained by fitting the indoor experimentally measured data. The indoor experimentally measured mineral volume content and porosity were taken as the input conditions to solve the biot coefficient (α), which is the ratio of formation pore space deformation to total volume change. The biot coefficient (α) is calculated according to the following formula:

$$\alpha = 1 - K_{\mathrm{dry}}/K_m \tag{7}$$

where K_{dry} is the bulk modulus of dry rock, GPa; K_m is the bulk modulus of mineral, GPa.

Then the biot coefficient was linearly fitted with the active porosity to obtain the expression of the biot coefficient of tight sandstone reservoir:

$$\alpha = 0.386 \cdot \ln(\varphi_{\text{eff}}) + 1.743 \tag{8}$$

where α is biot coefficient, dimensionless; Φeff is the active porosity of tight sandstone, %. The active porosity was calculated according to the logging curve in order to calculate the biot coefficients of single wells in the whole area and modeled work area.

Finally, the maximum horizontal in-situ stress and minimum horizontal in-situ stress were calculated according to the following formula based on the rock parameters, biot coefficient and pore pressure:

$$\begin{aligned}\sigma_h &= \frac{\nu}{1-\nu}(\sigma_v - \alpha P_p) + \frac{E\xi_h}{1-\nu^2} + \frac{\nu E\xi_H}{1-\nu^2} + \alpha P_P \\ \sigma_H &= \frac{\nu}{1-\nu}(\sigma_v - \alpha P_p) + \frac{E\xi_H}{1-\nu^2} + \frac{\nu E\xi_h}{1-\nu^2} + \alpha P_P\end{aligned} \tag{9}$$

where σH is the maximum horizontal principal stress, MPa; σh is the minimum horizontal principal stress, MPa; υ is Poisson's ratio, dimensionless; σv is the overburden pressure, MPa; α is biot coefficient, dimensionless; Pp is pore pressure, MPa; E is Young's modulus, GPa; εh and εH are the strain in the direction of minimum and maximum horizontal principal stress obtained by fitting the experimental data, respectively, dimensionless.

According to the measure in-situ stress of the tight sandstone reservoir in the north of Songliao Basin, the error of the calculated in-situ stress was analyzed. The error is the ratio of the difference between the calculated stress and the indoor experimentally measured stress to the measured stress. The error analysis shows that the overall error of vertical stress is within 5%, meeting the error requirement. However, the calculated minimum horizontal stress of G2, G4 and G5 wells and the calculated maximum horizontal stress of G5 well have large errors (more than 5%). Thus, the calculation of in-situ stress is a complex technical task. At present, there is no calculation formula suitable for all wells in one area. These calculation formulas are always called in-situ stress calculation models. The results calculated according to the formulas deviate from the actual in-situ stress value and thus will be corrected by other methods (Table 1).

In order to avoid the deviation between the calculated maximum and minimum horizontal stress, the implicit relationship between the in-situ stress of the reservoir and the conventional logging data was established by using the calibration and prediction advantages of BP neural network in order to form a new in-situ stress prediction model in the area. The correlation analysis between the measured stress data points of the core in the area and the conventional logging curves (P-wave slowness, neutron logging curve, density logging curve, gamma-ray logging curve) and depth attributes show that the total correlation coefficient between the sample data and the input layer is more than 91%. Thus, these logging parameters can be used as learning sample data for machine learning.

The area has some problems, such as only 48 in-situ stress measurement data points, few learning samples, discontinuous data, multiple solutions, and random data between

Table 1. Error of Calculated In-situ Stress

Well No.	Error of calculated in-situ stress			
	Depth range (m)	Relative error of vertical stress (%)	Relative error of maximum horizontal stress (%)	Relative error of minimum horizontal stress (%)
G1	1773–1875	0.63	2.82	2.87
G2	2015–2100	0.30	3.29	5.24
G3	2015–2110	2.24	2.04	3.27
G4	1793–1886	0.83	3.75	5.02
G5	1996–2141	1.13	8.05	7.63
Average	-	0.90	3.99	4.86

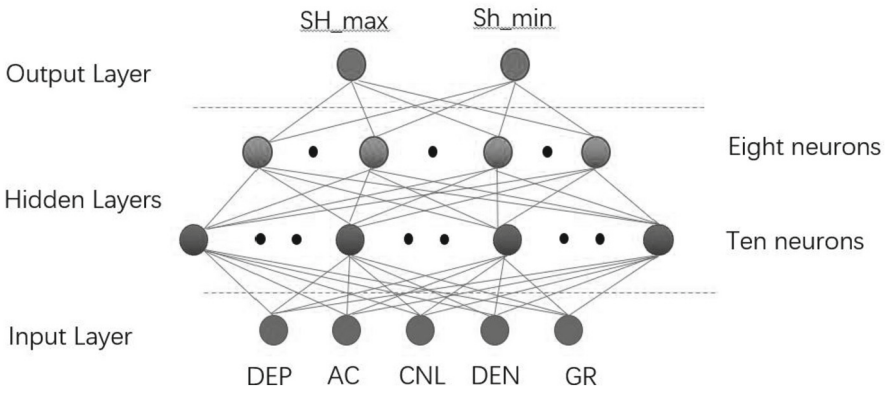

Fig. 1. Prediction of single well in-situ stress by BP neural network

measurement points. In order to solve the above problems, the neural network method calculation formula method were organically combined together, i.e. the continuous data of the wells with small errors in the calculated in-situ stress results were used as the sample data of machine learning, to extend the sample data from small core (discontinuous) samples to large logging (continuous) samples, further reduce the possibility of multiple prediction results and thus keep a good correlation between the prediction result and logging curve. Specifically, the continuous vertical stress, calculated maximum and minimum horizontal stress of G1 well and G3 well at different depths with the error of calculated stress value within 3% were selected to extend the data of 48 measured in-situ stress parameters (small samples) and thus form large sample (learning sample) data; the vertical in-situ stress, maximum horizontal stress and minimum horizontal stress of tight sandstone oil and gas wells were calculated by BP neural network model using the geophysical logging (acoustic logging, neutron logging, density logging, gamma-ray logging) curve of single well and depth value as training samples. After determination of the above training input parameters of machine learning, the BP neural network model

(as shown in Fig. 7) consisting of one input layer, two hidden layers and one output layer built by matlab was used to select Levenberg-Marquardt backpropagation for training and predict the maximum and minimum horizontal principal stress of G2, G4 and G5 wells. Tables 5–6 are obtained through error statistics. The error analysis shows that the maximum horizontal principal stress and the minimum horizontal principal stress predicted by BP neural network based on the indoor experimentally measured data have the average error of 4.73% and 10.28%, respectively. Compared with the error of the calculated in-situ stress, the error doesn't reduce. The maximum and minimum horizontal principal stresses predicted by BP neural network based on the extended large sample have the average error of 1.54% and 1.45%, respectively. The prediction by BP neural network model shows that the extended large sample has much smaller error than the small sample. Therefore, the calculated in-situ stresses of the wells with small error were used to extend the learning sample of the indoor experimentally measured data and thus change the small sample into a large sample for prediction by BP neural network. Thus, the prediction result is more accurate. This method can be used to predict and comprehensively evaluate the in-situ stress of other wells in this area.

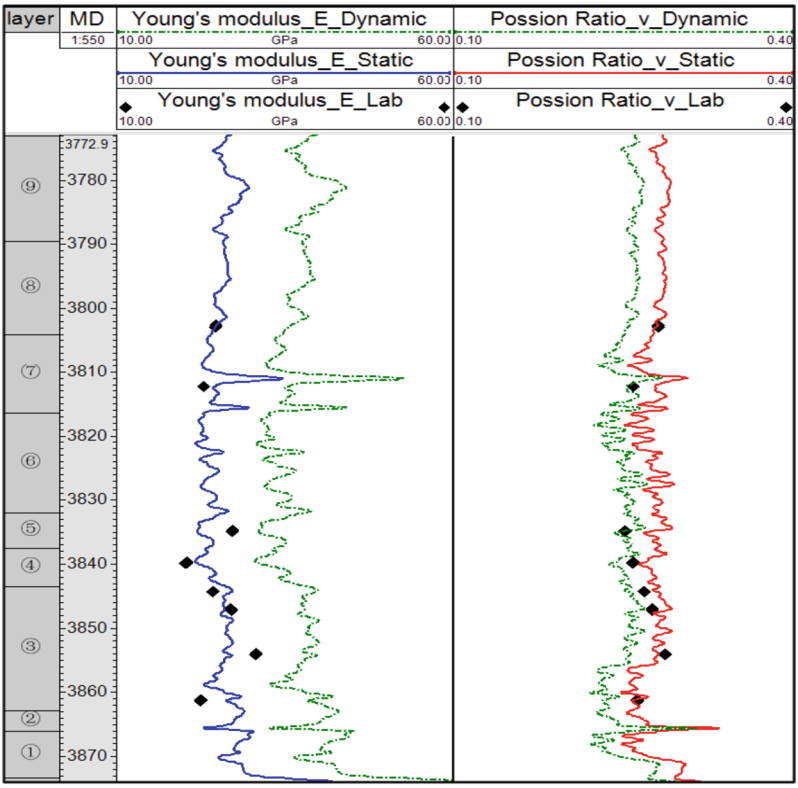

Fig. 2. Indoor measured and Calculation of dynamic-static Poisson's ratio or Young's modulus based on logging curve

Table 2. Comparison of errors of the in-situ stress predicted by neural network models based on different learning samples

Well No.	Error of the in-situ stress predicted by formula method (%)		Error of the in-situ stress predicted by BP neural network only based on indoor experimentally measured data (%)		Error of the in-situ stress predicted by BP neural network based on extended large samples (%)	
	Maximum horizontal stress	Minimum horizontal stress	Maximum horizontal stress	Minimum horizontal stress	Maximum horizontal stress	Minimum horizontal stress
G2	3.29	5.24	5.23	12.07	0.16	0.21
G4	3.75	5.02	4.54	10.86	3.61	3.34
G5	8.05	7.63	4.42	7.93	0.85	0.80
Average error	5.03	5.96	4.73	10.28	1.54	1.45

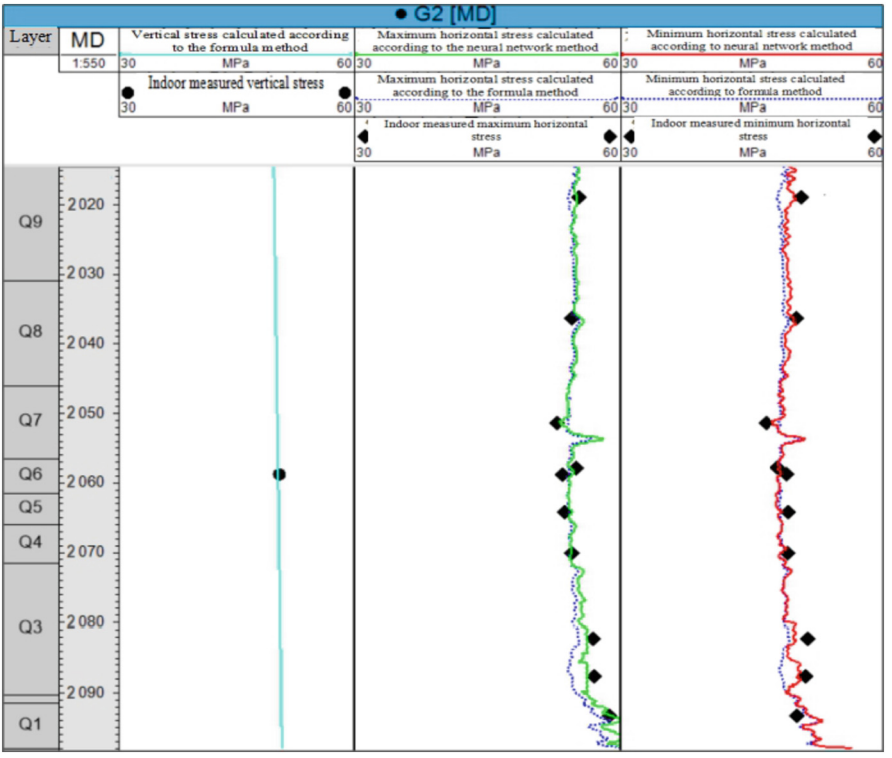

Fig. 3. Comparison between the calculated results of the three-dimensional stress neural network and the measured values

3 Results and Discussions

The above method can further extend the establishment of in-situ stress geological model, i.e. the fine geological model was created by using log and seismic data first and then the acoustic wave slowness curves, neutron logging curves, density logging curves, and gamma-ray logging curves of 5 wells in the area were discretized to obtain the averages of each layer in each well. The area has large area and only 5 wells, so the co-kriging interplotation algorithm was used for spatial interpolation to obtain the spatial distribution characteristics of different parameters.

The interpretation results of the above-mentioned in-situ stress were discretized to obtain the correlation between statistical data points and conventional logging curves (acoustic wave slowness logging curve, neutron logging curve, density logging curve, gamma-ray logging curve) and depth attribute model. The neural network algorithm shows that the total correlation coefficient exceeds 0.98. Therefore, it is feasible to use these logging parameter models as learning data and the measured in-situ stress as sample data for machine learning.

	AC	CNL	DEN	GR	dep	svvv
AC	1.0000	0.7065	0.0676	0.1852	0.4516	0.4665
CNL	0.7065	1.0000	0.5923	0.1591	0.0194	0.0294
DEN	0.0676	0.5923	1.0000	0.5683	0.5692	0.5801
GR	0.1852	0.1591	0.5683	1.0000	0.2466	0.2522
dep	0.4516	0.0194	0.5692	0.2466	1.0000	0.9856
Total	0.8567	0.8954	0.8999	0.6793	0.7923	0.9932

(a. Correlation between vertical stress and different logging parameter models)

	AC	CNL	DEN	GR	dep	SHmaxsjwn [for shmaxsjwn]
AC	1.0000	0.7065	0.0676	0.1852	0.4516	0.2920
CNL	0.7065	1.0000	0.5923	0.1591	0.0194	0.1948
DEN	0.0676	0.5923	1.0000	0.5683	0.5692	0.5905
GR	0.1852	0.1591	0.5683	1.0000	0.2466	0.1766
dep	0.4516	0.0194	0.5692	0.2466	1.0000	0.9463
Total	0.8567	0.8954	0.8999	0.6793	0.7923	0.9827

(b. Correlation between maximum horizontal stress and different logging parameter models)

	AC	CNL	DEN	GR	dep	SHminsjwn [for shminsjwn]
AC	1.0000	0.7065	0.0676	0.1852	0.4516	0.3298
CNL	0.7065	1.0000	0.5923	0.1591	0.0194	0.1224
DEN	0.0676	0.5923	1.0000	0.5683	0.5692	0.5706
GR	0.1852	0.1591	0.5683	1.0000	0.2466	0.1917
dep	0.4516	0.0194	0.5692	0.2466	1.0000	0.9687
Total	0.8567	0.8954	0.8999	0.6793	0.7923	0.9863

(c. Correlation between minimum horizontal stress and different logging parameter models)

Fig. 4. Spatial Distribution Model of Logging Parameters

The models of vertical stress, maximum horizontal stress and minimum horizontal stress were created by neural network algorithm. The in-situ stress prediction shows that the study area has the characteristics of maximum horizontal principal stress > vertical principal stress > minimum horizontal principal stress, i.e. Class III in-situ stress in the state of sliding stress, and always form vertical fractures after fracturing. Therefore, the area can be developed by horizontal well + fracturing; the horizontal well trend is perpendicular to the direction of the maximum horizontal stress, so the north-north-east well spacing is suggested. The study on the stress difference distribution shows that due to relatively large stress difference in the axial region and anticline, intensive cut fracturing of horizontal wells is suitable for the large stress blocks to improve the producing degree; the basal leaf cross has smaller stress difference than the anticline,

so large cluster distance fracturing is suitable for small stress blocks to form complex artificial fractures and expand the swept volume.

4 Conclusions

Compared with the existing technology, this method has the following beneficial effects: (1) By comprehensively using core analysis data, indoor measured mechanical data, conventional logging data, XMAC logging data, etc., the method for prediction of one-dimension, two-dimension and three-dimension in-situ stress prediction integrating artificial intelligence and traditional geomechanics was innovatively put forward based on research on structure, sedimentary facies and reservoir properties in order to extend small core samples to large logging samples; (2) by creating a neural network-based three-dimensional in-situ stress prediction model, the spatial in-situ stress distribution of tight sandstone reservoirs in the test area was predicted and analyzed. The relative error between the predicted in-situ stress and the measured result is within 3%, indicating that the method improves the prediction accuracy of in-situ stress in the study area. Thus, the research results provide an important basis for the design of integrated geological engineering scheme. In conclusion, this method is very worthy of application in stress prediction technology for tight sandstone reservoirs due to its advantages, including simple logic, accuracy and reliability.

References

1. Boswell, L.F., Chen, Z.: A general failure criterion for plain concrete. Int. J. Solids Struct. **23**(5), 621–630 (1987)
2. Cai, W., Zhu, H., Liang, W., Zhang, L., Wu, W.: A new version of the generalized Zhang–Zhu strength criterion and a discussion on its smoothness and convexity. Rock Mech. Rock Eng. 1–17 (2021)
3. Colmenares, L.B., Zoback, M.D.: A statistical evaluation of intact rock failure criteria constrained by polyaxial test data for five different rocks. Int. J. Rock Mech. Min. Sci. **39**(6), 695–729 (2002)
4. Jiang, J., Pietruszczak, S.: Convexity of yield loci for pressure sensitive materials. Comput. Geotech. **5**(1), 51–63 (1988)
5. Kim, M.K., Lade, P.V.: Modelling rock strength in three dimensions. Int. J. Rock Mech. Min. Sci. Geomech. Abstracts **21**(1), 21–33. Pergamon (1984)
6. Lee, Y.K., Pietruszczak, S., Choi, B.H.: Failure criteria for rocks based on smooth approximations to Mohr-Coulomb and Hoek-Brown failure functions. Int. J. Rock Mech. Min. Sci. **56**, 146–160 (2012)
7. Li, C., Li, C., Zhao, R., Zhou, L.: A strength criterion for rocks. Mech. Mater. **154**(3), 1–9 (2021)
8. Lade, P.V., Duncan, J.M.: Elastoplastic stress-strain theory for cohesionless soil. J. Geotech. Eng. Div. **101**(10), 1037–1053 (1975)
9. Pan, X.D., Hudson, J.A.: A simplified three-dimensional Hoek-Brown yield criterion. In: ISRM International Symposium. OnePetro (1988)
10. Priest, S.D.: Determination of shear strength and three-dimensional yield strength for the Hoek-Brown criterion. Rock Mech. Rock Eng. **38**(4), 299–327 (2005)

11. Yu, M., Zan, Y., Xu, S.: Rock Strength Theory and Its Application. Science Press (2017). (in Chinese)
12. Zan, Y., Yu, M., Wang, S.: Nonlinear unified strength criterion of rock. Chin. J. Rock Mech. Eng. **21**(10), 1435–1441 (2002). (in Chinese)
13. Zan, Y., Yu, M., Zhao, J.: Nonlinear unified strength theory of rock under high stress state. Chin. J. Rock Mech. Eng. **23**(13), 2143–2148 (2004). (in Chinese)
14. Zan, Y., Yu, M.: Generalized Nonlinear Unified Strength Theory of Rock. J. Southwest Jiaotong Univ. **48**(4), 616–624 (2013). (in Chinese)
15. Zhang, Q., Zhu, H., Zhang, L.: Modification of a generalized three-dimensional Hoek-Brown strength criterion. Int. J. Rock Mech. Min. Sci. **59**, 80–96 (2013)